JOURNAL OF THERMOPHYSICS AND HEAT TRANSFER
Vol. 20, No. 3, July–September 2006

Optimal Inverse Design Problem in Determining Cooling Conditions for High-Speed Motors

Cheng-Hung Huang* and Hung-Chi Lo†
National Cheng Kung University, Tainan 701, Taiwan, Republic of China

The effective optimal and practical time-dependent heat transfer coefficients of the cooling passage for high-speed motors are determined in a three-dimensional optimal control problem. The control algorithm utilizing the steepest descent method and a general purpose commercial code CFX4.4 is applied successfully in accordance with the design (or desired) temperature distributions on the interior heating surface. Two different design temperature distributions are used to illustrate the validity of determining both the effective optimal and practical heat transfer coefficients. Results of the numerical simulation show that the reliable estimated effective practical heat transfer coefficients can be obtained by using the present optimal inverse design (or optimal control) algorithm.

Nomenclature

Cp	=	heat capacity
h_w	=	heat transfer coefficient for water (control function)
h_∞	=	heat transfer coefficient for ambient air
$J[h_w(S_c, t)]$	=	functional defined by Eq. (2)
$J'[h_w(S_c, t)]$	=	gradient of functional defined by Eq. (14)
k	=	thermal conductivity
$P^n(S_c, t)$	=	direction of descent defined by Eq. (4)
q	=	heat flux generated by electric motor in rotor and stator
$T(\Omega, t)$	=	estimated temperatures
$Y(S_q, t)$	=	design temperature
β	=	search step size
$\Delta T(\Omega, t)$	=	sensitivity function defined by Eq. (5)
ε	=	convergence criteria
$\lambda(\Omega, t)$	=	Lagrange multiplier defined by Eq. (11)
ρ	=	density

Subscripts

c	=	cooling surface
e	=	design temperature indicating point
q	=	heating surface

Superscript

n	=	iteration index

I. Introduction

TO achieve the goal of higher productivity, it is always necessary to maintain a high speed in the drive system of a machine tool, such as the motor. For this reason, high-speed machining is a promising technology because it can drastically increase productivity while reducing the production costs.

The technology of high-speed motors is still relatively new. Not much work regarding the study of the thermal performance of high-speed motors has been proposed. A qualitative power flow model is presented by Bossmanns and Tu[1] to characterize the power distribution of a high-speed motorizedspindle. Quantitative heat source models of the built-in motor and the bearings were then developed. These models are verified with a custom-built high-performance motorized spindle. Yang et al.[2] proposed a new measurement method for spindle thermal errors in a machine tool based on the use of a ball bar system instead of the conventional capacitance sensor system. The novel measurement method is more efficient and easier to use compared to conventional measurement systems. The characterizing and modeling of the thermal growth of a motorized high-speed spindle was reported by Chen and Hsu.[3] It was found that the displacement-based thermal error model has much better accuracy and robustness than the temperature-based model. Ohishi and Matsuzaki[4] presented a report on the first stage of research on the thermal analysis of spindle units with aerostatic bearings and an experimental investigation of temperature distributions. The experimental results show that the heat flow pattern is essentially radial flow, although axial heat flow was observed and the temperatures are proportional to the square of the spindle speed. For all of the preceding references, the working conditions are given; thus, they did not represent design problems.

A higher speed inevitably increases the thermal effects on the machine tool itself, thereby resulting in thermal failures or distortions of the machine components associated with the generated heat sources. The major heat sources within the spindle system can be composed of the following four items[1]: 1) heat generation by ball bearings, 2) heat generation by the electric motor in the rotor and stator, 3) heat generation due to viscosity shear of air by the rotating components of the spindle, and 4) a qualitative description of power distribution from spindle heat sources to heat sinks.

Eventually, the thermal effect causes 1) spindle failures or 2) dimensional and geometrical errors in the machined work piece due to a mismatch between the tool and the work piece. Because thermally induced errors have a direct impact on component life, the surface finish, and the geometric shape of the finished work piece, control of thermal effect becomes critical to the high-speed motor.

To alleviate the heat generation by the electric motor in the rotor and stator, a cooling passage in the motor housing is often built in. By variation of the heat transfer coefficient of the cooling passage, the temperature distributions of the motor housing can be controlled. The objective of this study is as follows: By utilization of an optimal inverse design algorithm, the steepest descent method (SDM), and design temperature distribution on the heating surface, the effective optimal and practical time-dependent heat transfer coefficients of the cooling passage for motors are estimated.

The thermal design or control problems using a gradient algorithm can be found in the open literature. Meric[5,6] used the conjugate gradient method to find the optimal boundary control temperatures for a nonlinear system, that is, temperature-dependent thermal properties. Chen and Ozisik used a similar algorithm to determine the optimal heating sources for a slab[7,8] and a cylinder[9] in a nonlinear optimal control problem. Huang[10] solved a similar optimal control

Received 17 May 2005; revision received 19 September 2005; accepted for publication 26 September 2005.

*Professor, Department of Systems and Naval Mechatronic Engineering; chhuang@mail.ncku.edu.tw.

†Graduate Student, Department of Systems and Naval Mechatronic Engineering.

problem using a conjugate gradient method. Recently, Huang and Li[11] solved a three-dimensional optimal control problem to determine the optimal boundary control heat fluxes.

The three-dimensional thermal inverse design problems for an irregular domain are still limited in the literature. To the authors' knowledge, the three-dimensional design problem in estimating both the effective optimal and practical heat transfer coefficients for high-speed motors with complicated (or real) motor geometry has never been examined. The objective of this study is to extend the techniques used in Refs. 10 and 11 to a transient three-dimensional optimal control problem in estimating the effective time-dependent heat transfer coefficient of the cooling passage.

The SDM derives its basis from the perturbational principle[12] and transforms the inverse problem to the solution of three problems, namely, the direct problem, the sensitivity problem, and the adjoint problem, which will be discussed in detail in the text.

II. Direct Problem

The typical housing model for a high-speed motor is shown in Fig. 1. A screw-type cooling passage was built inside the housing to allow cooling enhancement and to avoid thermal failures and distortions. All of the external surfaces S_e, except for the right and left surfaces, S_r and S_l, are subjected to a convective boundary condition with a prescribed heat transfer coefficient h_∞ and an ambient temperature T_∞. The right and left surfaces, S_r and S_l, are assumed to have an adiabatic condition. A known heat flux q generated by the electric motor in the rotor and stator is imposed on the internal heating surface S_q, and the internal surfaces elsewhere, S_i, are assumed to have an adiabatic condition. The boundary condition inside the cooling passage S_c is subjected to a convective boundary condition with a prescribed heat transfer coefficient $h_w(S_c, t)$ and a water temperature T_w.

Figure 2a shows in detail the geometry and dimensions of the motor housing, and Fig. 2b shows the grid system of the motor housing. The formulation of this three-dimensional transient heat conduction problem can be expressed as

$$k\left[\frac{\partial^2 T(\Omega,t)}{\partial x^2}+\frac{\partial^2 T(\Omega,t)}{\partial y^2}+\frac{\partial^2 T(\Omega,t)}{\partial z^2}\right]=\rho Cp\frac{\partial T(\Omega,t)}{\partial t} \quad (1a)$$

in (Ω, t),

$$k\frac{\partial T}{\partial n}=0 \quad (1b)$$

on the right and left surfaces S_r and S_l,

$$-k\frac{\partial T(S_q,t)}{\partial n}=q \quad (1c)$$

on the heating surface S_q,

$$k\frac{\partial T}{\partial n}=0 \quad (1d)$$

on the internal surface S_i (except for the heating surface S_q),

$$-k\frac{\partial T(S_e,t)}{\partial n}=h_\infty(T-T_\infty) \quad (1e)$$

on the external surfaces S_e,

$$-k\frac{\partial T(S_c,t)}{\partial n}=h_w(S_c,t)(T-T_w) \quad (1f)$$

on the cooling passage surfaces S_c, and

$$T(\Omega,t)=T_0, \qquad \text{for} \qquad t=0 \quad (1g)$$

Here Cp is the heat capacity of the motor housing; h_∞ and T_∞ are the ambient heat transfer coefficient and temperature, respectively; $h_w(S_c, t)$ and T_w are the heat transfer coefficient and water temperature inside the cooling passage of the motor housing; q is the heat flux generated by the electric motor in the rotor and stator; and T_0 is the initial temperature.

The direct problem considered here is concerned with calculating the motor housing temperature distributions when the heat flux q, heat transfer coefficients h_∞ and $h_w(S_c, t)$, and thermal properties, as well as the initial and boundary conditions, are all known. The solution for the preceding three-dimensional energy equation in the domain $\Omega(x, y, z)$ is solved using CFX4.4 and its FORTRAN subroutine USRBCS.

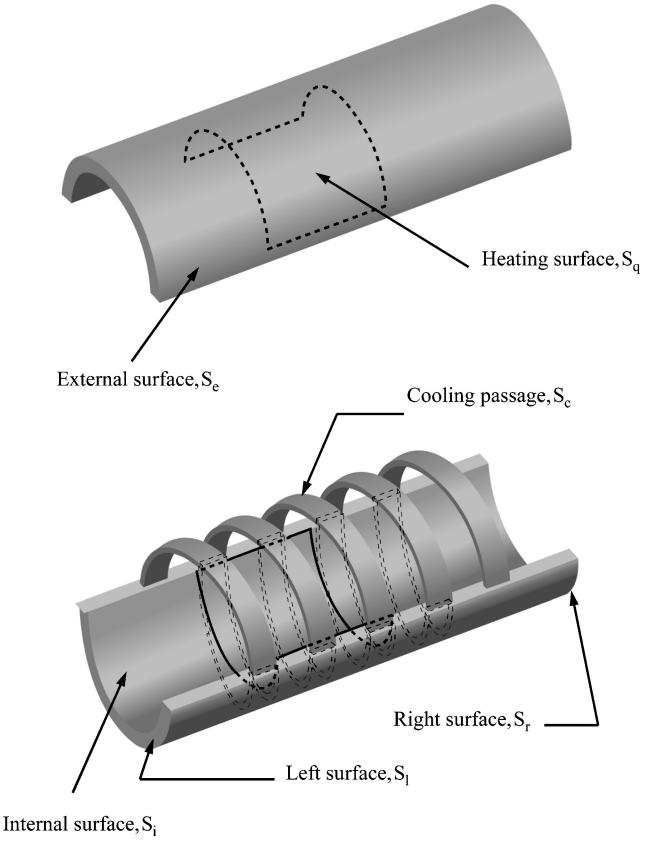

Fig. 1 Geometry of housing for motors.

III. Optimal Control Problem

For the optimal control problem considered here, the time-dependent heat transfer coefficient $h_w(S_c, t)$, that is, the control function, is regarded as being unknown, but everything else in Eq. (1) is known. In addition, the design (or desired) temperature distributions on the internal heating surface S_q are available.

Let the design temperature on the heating surface S_q be denoted by $\boldsymbol{Y}(S_q, t) \equiv \boldsymbol{Y}(x_q, y_q, z_q, t) \equiv Y_e(S_q, t)$, let $e = 1$–E, and let E represent the total number of design temperature indicating points (or grid points). This design problem can be stated as follows: By utilization of the aforementioned design temperature distribution $Y_e(S_q, t)$, estimate the optimal time-dependent heat transfer coefficient $h_w(S_c, t)$.

The solution of this optimal control problem is to be obtained in such a way that the following functional is minimized:

$$J[h_w(S_c,t)]=\int_{t=0}^{t_f}\sum_{e=1}^{E}[T_e(S_q,t)-Y_e(S_q,t)]^2\,\mathrm{d}t \quad (2)$$

here $T_e(S_q, t)$ are the estimated or computed temperatures at the design temperature indicating locations (x_q, y_q, z_q) and time t. These quantities are determined from the solution of the direct problem given earlier by using the estimated optimal time-dependent heat transfer coefficient $h_w(S_c, t)$.

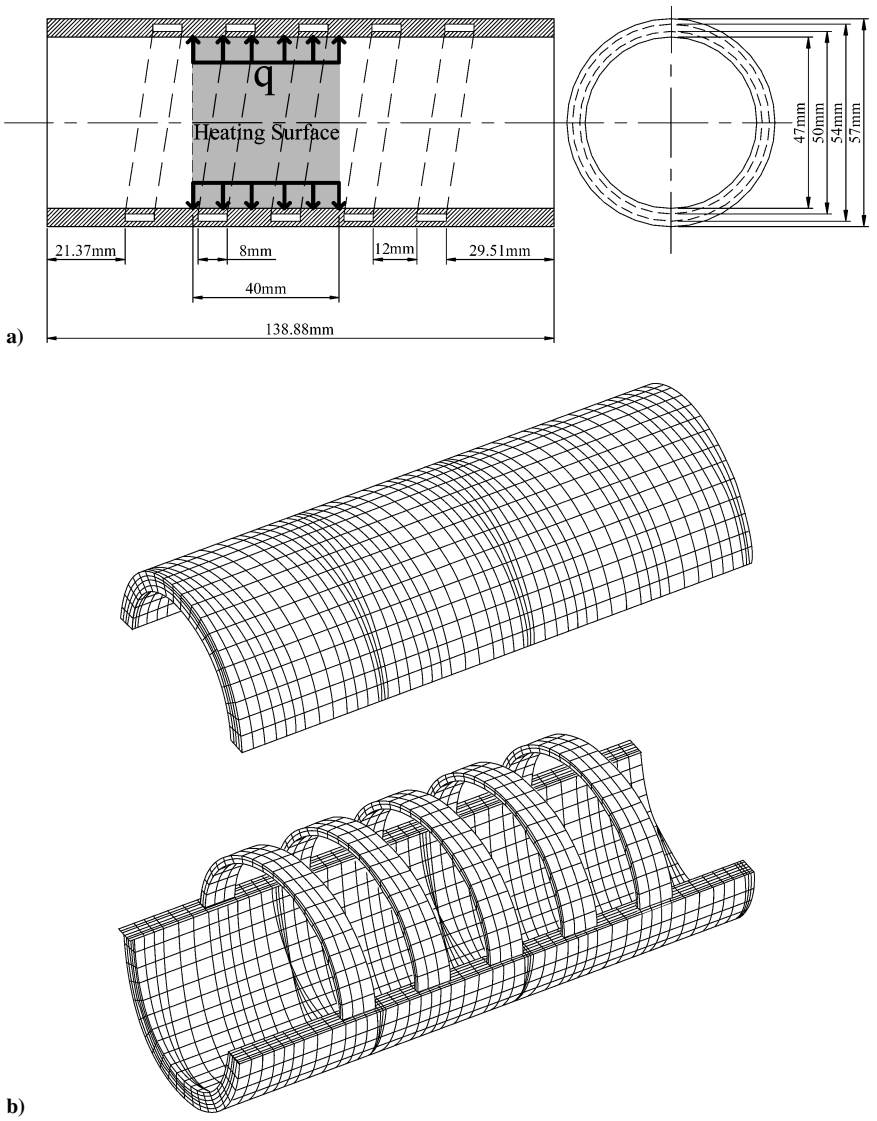

Fig. 2 Housing a) dimensions and b) grid system.

IV. SDM for Minimization

An iterative process based on the following SDM[12] is now applied for the estimation of optimal time-dependent heat transfer coefficient $h_w(S_c, t)$ by minimizing the functional $J[h_w(S_c, t)]$

$$h_w^{n+1}(S_c, t) = h_w^n(S_c, t) - \beta^n P^n(S_c, t), \qquad \text{for} \qquad n = 0, 1, 2, \ldots \tag{3}$$

Here β^n is the search step size in going from iteration n to iteration $n+1$ and $P^n(S_c, t)$ is the direction of descent, that is, search direction, given by

$$P^n(S_c, t) = J'^n(S_c, t) \tag{4}$$

This is also the gradient direction at iteration n for the SDM. To complete the iterations in accordance with Eq. (3), the step size β^n and the gradient of the functional $J'^n(S_c, t)$ need be computed. To develop expressions in determining these two quantities, a sensitivity problem and an adjoint problem need be constructed as described hereafter.

A. Sensitivity Problem and Search Step Size

It is assumed that when $h_w(S_c, t)$ undergoes a variation Δh_w, then T is perturbed by $T + \Delta T$. Then by replacement in the direct problem of h_w by $h_w + \Delta h_w$ and of T by $T + \Delta T$, subtraction of the direct problem from the resulting expressions, and by neglecting the second-order terms, the following sensitivity problem for the sensitivity function ΔT is obtained:

$$k\left[\frac{\partial^2 \Delta T(\Omega, t)}{\partial x^2} + \frac{\partial^2 \Delta T(\Omega, t)}{\partial y^2} + \frac{\partial^2 \Delta T(\Omega, t)}{\partial z^2}\right] = \rho Cp \frac{\partial \Delta T(\Omega, t)}{\partial t} \tag{5a}$$

in (Ω, t),

$$k\frac{\partial \Delta T}{\partial n} = 0 \tag{5b}$$

on the right and left surfaces S_r and S_l,

$$-k\frac{\partial \Delta T(S_q, t)}{\partial n} = 0 \tag{5c}$$

on the heating surface S_q,

$$k\frac{\partial \Delta T}{\partial n} = 0 \tag{5d}$$

on the internal surface S_i (except for the heating surface S_q),

$$-k\frac{\partial \Delta T(S_e, t)}{\partial n} = h_\infty \Delta T \tag{5e}$$

on the external surfaces S_e,

$$-k\frac{\partial \Delta T(S_c,t)}{\partial n} = \Delta h_w(T - T_w) + h_w \Delta T \tag{5f}$$

on the cooling passage surfaces S_c and

$$\Delta T(\Omega, t) = 0, \qquad \text{for} \qquad t = 0 \tag{5g}$$

CFX 4.4 is used to solve the foregoing sensitivity problem. The functional $J[h_w^{n+1}(S_c,t)]$ for iteration $n+1$ is obtained by rewriting Eq. (2) as

$$J\left[h_w^{n+1}(S_c,t)\right] = \int_{t=0}^{t_f}\sum_{e=1}^{E}\left[T_e\left(S_q,t;h_w^n-\beta^n P^n\right) - Y_e(S_q,t)\right]^2 \mathrm{d}t \tag{6}$$

where h_w^{n+1} is replaced by the expression given by Eq. (3). If temperature $T_e(S_q,t;h_w^n-\beta^n P^n)$ is linearized by a Taylor expansion, Eq. (6) takes the form

$$J\left[h_w^{n+1}(S_c,t)\right] = \int_{t=0}^{t_f}\sum_{e=1}^{E}\left[T_e\left(S_q,t;h_w^n\right) - \beta^n \Delta T_e\left(S_q,t;P^n\right) - Y_e(S_q,t)\right]^2 \mathrm{d}t \tag{7}$$

where $T_e(S_q,t;h_w^n)$ is the solution of the direct problem by using the estimated heat transfer coefficient on S_q. The sensitivity functions $\Delta T_e(S_q,t;P^n)$ are taken as the solutions of problem (5) at the design temperature indicating positions (x_q,y_q,z_q) and time t by using $\Delta h_w = P^n$. The search step size β^n is determined by minimizing the functional given by Eq. (7) with respect to β^n. The following expression results:

$$\beta^n = \frac{\int_{t=0}^{t_f}\sum_{e=1}^{E}[T_e(S_q,t) - Y_e(S_q,t)]\Delta T_e(S_q,t)\,\mathrm{d}t}{\int_{t=0}^{t_f}\sum_{e=1}^{E}[\Delta T_e(S_q,t)]^2\,\mathrm{d}t} \tag{8}$$

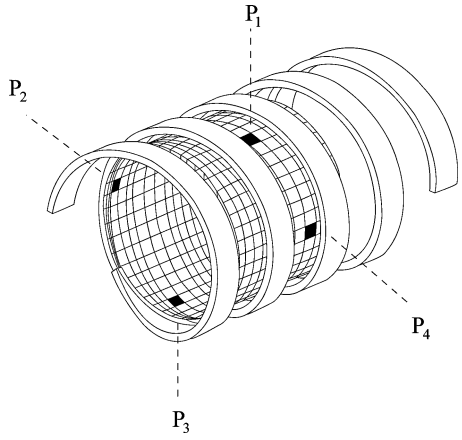

Fig. 3 Four specified locations for illustrated results.

B. Adjoint Problem and Gradient Equation

To obtain the adjoint problem, Eq. (1a) is multiplied by the Lagrange multiplier (or adjoint function) $\lambda(\Omega,t)$, and the resulting expression is integrated over the correspondent space and time domains. Then the result is added to the right-hand side of Eq. (2)

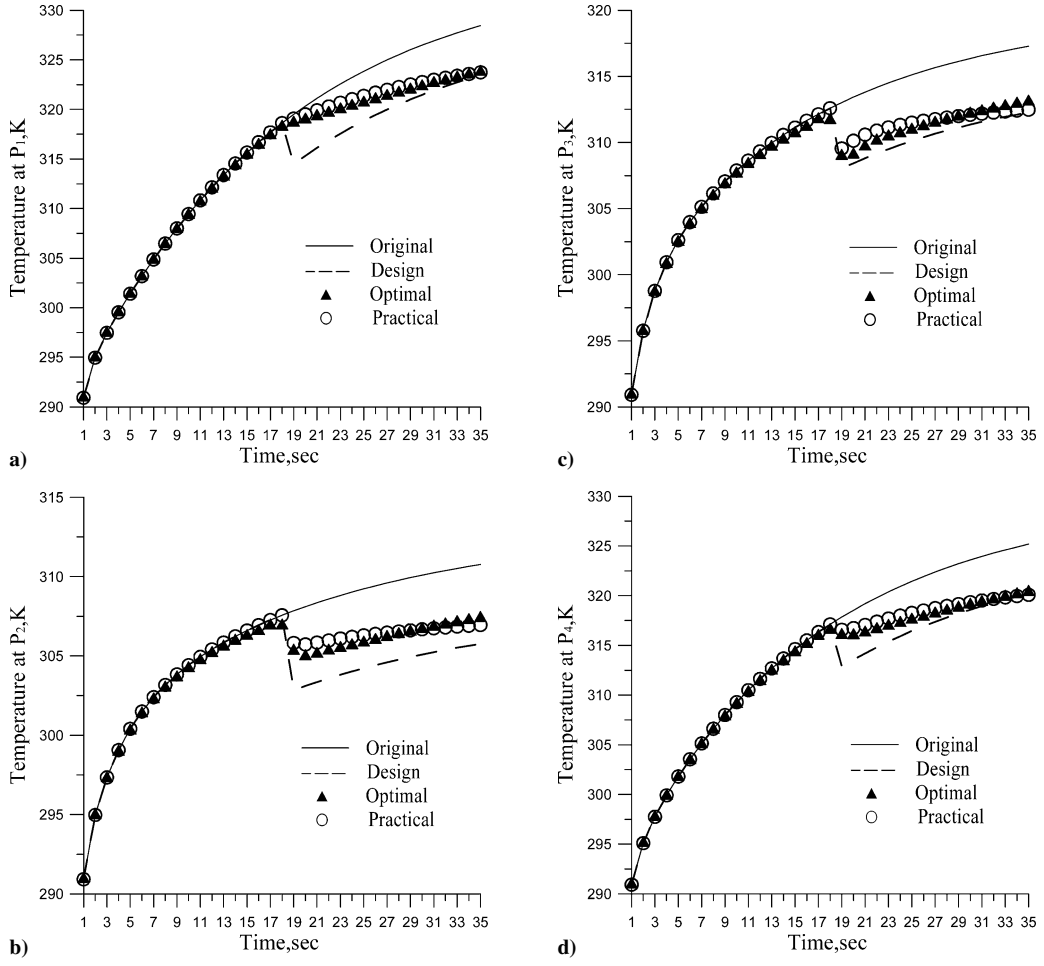

Fig. 4 Temperature distributions with time at a) P_1, b) P_2, c) P_3, and d) P_4 in case 1.

to yield the following expression for the functional $J[h_w(S_c, t)]$:

$$J[h_w(S_c,t)] = \int_{t=0}^{t_f} \sum_{e=1}^{E} [T_e(S_q,t) - Y_e(S_q,t)]^2 \, \mathrm{d}t$$

$$+ \int_{t=0}^{t_f} \int_{\Omega} \left[\lambda(\Omega,t) \times \left(\nabla^2 T - \frac{\rho Cp}{k} \frac{\partial T}{\partial t} \right) \right] \mathrm{d}\Omega \, \mathrm{d}t$$

$$= \int_{t=0}^{t_f} \int_{S_q} [T(S_q,t) - Y(S_q,t)]^2$$

$$\times \delta(x - x_q)\delta(y - y_q)\delta(z - z_q) \, \mathrm{d}S_q \, \mathrm{d}t$$

$$+ \int_{t=0}^{t_f} \int_{\Omega} \left[\lambda(\Omega,t) \times \left(\nabla^2 T - \frac{\rho Cp}{k} \frac{\partial T}{\partial t} \right) \right] \mathrm{d}\Omega \, \mathrm{d}t \qquad (9)$$

in (Ω, t), where $\delta(\,)$ is the Dirac delta function and where (x_q, y_q, z_q) refers to the design temperature indicating positions.

The variation ΔJ can be obtained by perturbing h_w by $h_w + \Delta h_w$ and T by $T + \Delta T$ in Eq. (9), subtracting the original Eq. (9) from the resulting expression, and neglecting the second-order terms. We, thus, find

$$\Delta J[h_w(S_c,t)] = \int_{t=0}^{t_f} \int_{S_q} 2[T(S_q,t) - Y(S_q,t)]$$

$$\times \Delta T \delta(x - x_q)\delta(y - y_q)\delta(z - z_q) \, \mathrm{d}S_q \, \mathrm{d}t$$

$$+ \int_{t=0}^{t_f} \int_{\Omega} \left[\lambda(\Omega,t) \times \left(\nabla^2 \Delta T - \frac{\rho Cp}{k} \frac{\partial \Delta T}{\partial t} \right) \right] \mathrm{d}\Omega \, \mathrm{d}t \qquad (10)$$

in (Ω, t).

In Eq. (10), the second double domain integral term is reformulated based on Green's second identity, the boundary conditions of the sensitivity problem given by Eqs. (5b–5e) are utilized, and then ΔJ is allowed to go to zero. The vanishing of the integrands containing ΔT leads to the following adjoint problem for the determination of $\lambda(\Omega, t)$:

$$k \left[\frac{\partial^2 \lambda(\Omega,t)}{\partial x^2} + \frac{\partial^2 \lambda(\Omega,t)}{\partial y^2} + \frac{\partial^2 \lambda(\Omega,t)}{\partial z^2} \right] + \rho Cp \frac{\partial \lambda(\Omega,t)}{\partial t} = 0 \qquad (11a)$$

in (Ω, t),

$$\frac{\partial \lambda}{\partial n} = 0 \qquad (11b)$$

on the right and left surfaces S_r and S_l,

$$\frac{\partial \lambda(S_q,t)}{\partial n} = 2(T - Y)\delta(x - x_q)\delta(y - y_q)\delta(z - z_q) \qquad (11c)$$

on the heating surface S_q,

$$\frac{\partial \lambda}{\partial n} = 0 \qquad (11d)$$

on the internal surface S_i (except for the heating surface S_q),

$$-k \frac{\partial \lambda(S_e,t)}{\partial n} = h_\infty \lambda \qquad (11e)$$

on the external surfaces S_e,

$$-k \frac{\partial \lambda(S_c,t)}{\partial n} = h_w(S_c,t)\lambda \qquad (11f)$$

on the cooling passage surfaces S_c, and

$$\lambda(\Omega,t) = 0, \qquad \text{for} \qquad t = t_f \qquad (11g)$$

Finally, the following integral term is left:

$$\Delta J = \int_{t=0}^{t_f} \int_{S_c} -\frac{\lambda(S_c,t)}{k} (T - T_w) \Delta h_w(S_c,t) \, \mathrm{d}S_c \, \mathrm{d}t \qquad (12)$$

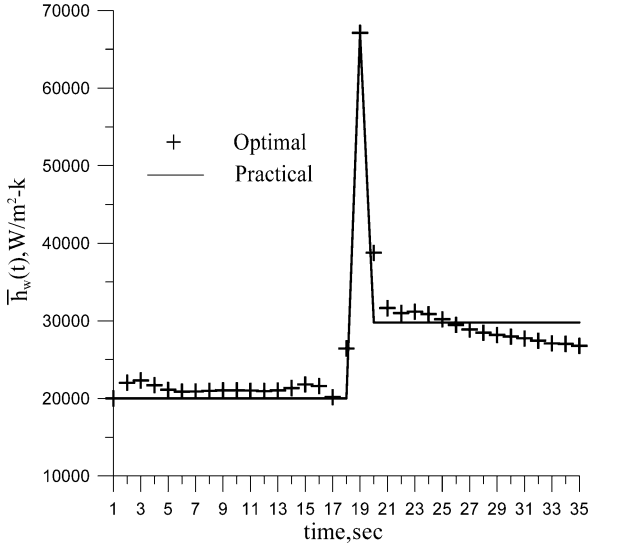

Fig. 5 Estimated effective optimal and practical heat transfer coefficients with time in case 1.

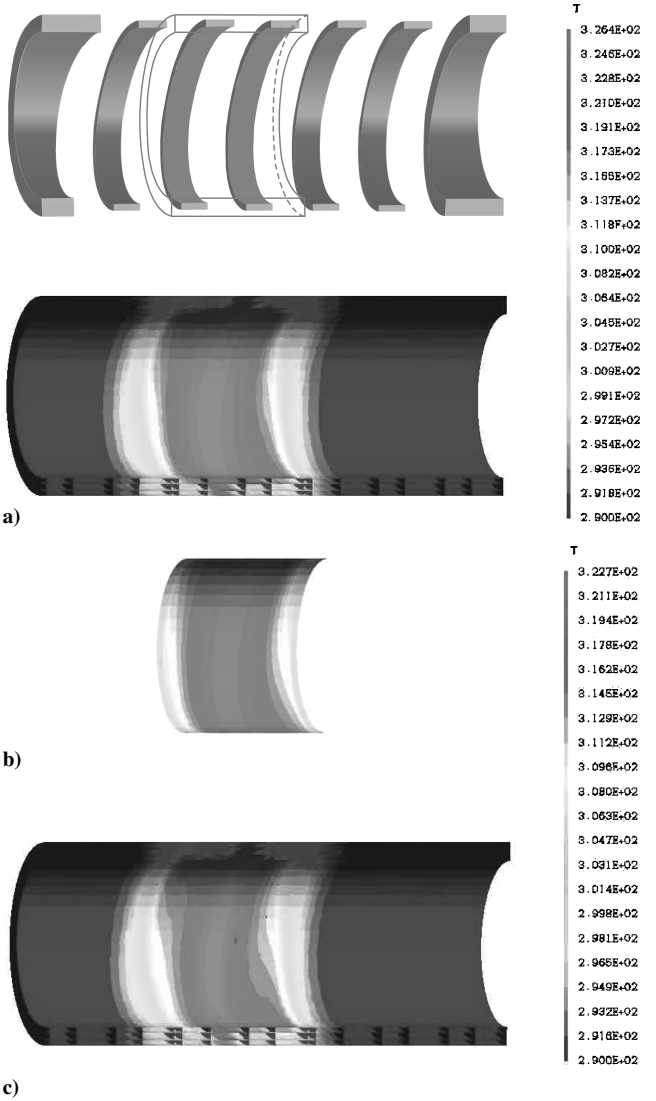

Fig. 6 Temperature distributions on internal surface of left housing at $t = 30$ s in case 1: a) original, b) design, and c) practical.

From definition (Ref. 12), the functional increment can be presented as

$$\Delta J = \int_{t=0}^{t_f} \int_{S_c} J'(S_c, t)\Delta h_w(S_c, t)\, \mathrm{d}S_c\, \mathrm{d}t \tag{13}$$

A comparison of Eqs. (12) and (13) leads to the following expression for the gradient of the functional $J[h_w(S_c, t)]$:

$$J'[h_w(S_c, t)] = -\{[\lambda(S_c, t)]/k\}(T - T_w) \tag{14}$$

on the cooling surfaces S_c.

C. Effective Optimal Heat Transfer Coefficient

Note in Eq. (3) that the estimated heat transfer coefficient $h_w(S_c, t)$ is a function of S_c; however, it is impossible to generate such a control function. Moreover, the estimated h_w on the heating surface side $S_{c,q}$ has the dominant effect because it is very close to the surface of assigning the design temperatures. To obtain an effective optimal control function, the average value of heat transfer coefficient over the heating surface side with time is, thus, used as the effective control function in this study, that is,

$$\bar{h}_w(t) = \sum_{i=1}^{N} h_{w,i}(S_{c,q}, t) \div N \tag{15}$$

Here N indicates the total number of grids on the surfaces $S_{c,q}$ and $\bar{h}_w(t)$ is the effective optimal heat transfer coefficient.

V. Computational Procedure

The computational procedure for the solution of this effective optimal control problem using the SDM may be summarized as follows. Suppose that $\bar{h}_w(t)$ is available at iteration n:

1) Solve the direct problem given by Eq. (1) for $T(\Omega, t)$.
2) Examine the value of the functional. Continue if it is greater than the stopping criterion ε.
3) Solve the adjoint problem given by Eq. (11) for $\lambda(\Omega, t)$.
4) Compute the gradient of the functional J' from Eq. (14).
5) Compute the direction of descent P^n from Eqs. (4).
6) Set $\Delta h_w = P^n$, and solve the sensitivity problem given by Eq. (5) for $\Delta T(\Omega, t)$.
7) Compute the search step size β^n from Eq. (8).
8) Compute the new estimation for h_w^{n+1} from Eq. (3) and the effective optimal heat transfer coefficient $\bar{h}_w(t)$ from Eq. (15).

Return to step 1.

VI. Results and Discussion

The time-dependent effective optimal heat transfer coefficient $\bar{h}_w(t)$, that is, the optimal control function for the high-speed motors, is to be estimated in this study using the SDM and desired temperature distributions with no prior information on the functional form of the control function.

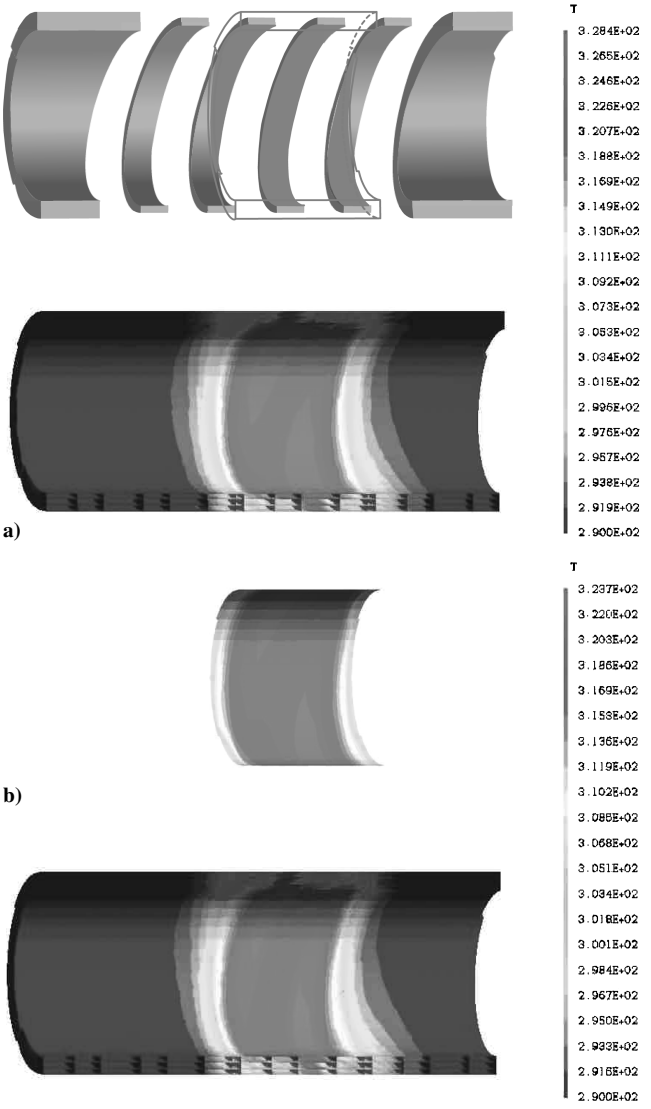

Fig. 7 Temperature distributions on internal surface of right housing at $t = 35$ s in case 1: a) original, b) design, and c) practical.

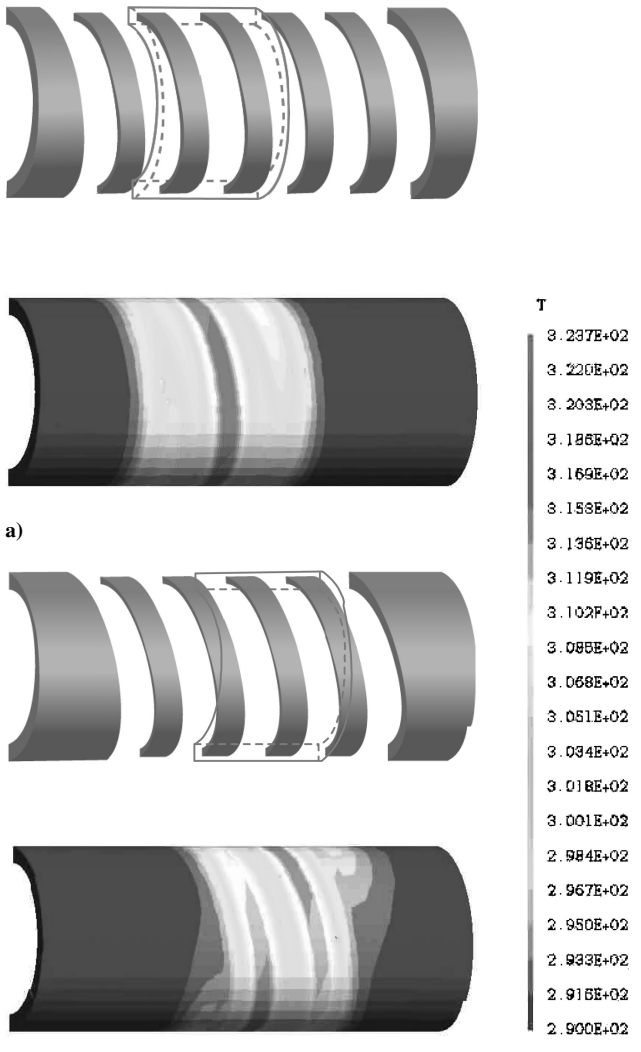

Fig. 8 External temperature distributions for a) left and b) right housing at $t = 35$ s in case 1.

The geometry of the motor housing is shown in Fig. 1. The dimensions and grid systems are shown in Fig. 2. The total number of grids in Ω, S_c, S_q, and $S_{c.q}$ are taken as 10,950; 1956; and 600, that is, $E = 600$, and 270, that is, $N = 270$, respectively. The design temperature indicating locations are at the grid points. The time period Δt is 1 s and total time t_f is 37 s, that is, there are 37 time steps. Therefore, there exist totally of 72,372 unknown discrete heat transfer coefficients in this study.

The physical model for this problem is described as follows: The material for the motor housing is American Iron and Steel Institute 302, and the thermal properties are taken as $k = 16.2$ W/(m · K), $\rho = 8000$ kg/m^3, and $Cp = 500$ J/kg · K. The ambient temperature and heat transfer coefficient are chosen as $T_\infty = 290$ K and $h_\infty = 30$ W/(m^2 · K), respectively. The initial temperature, water temperature, heat flux, and heat transfer coefficient for normal working conditions are taken as $T_0 = 290$ K, $T_w = 290$ K, $q = 40{,}000$ W/m^2, and $h_w(S_c, t) = 20{,}000$ W/(m^2 · K), respectively.

To illustrate the ability of the SDM to predict effective optimal heat transfer coefficient $\bar{h}_w(t)$ with optimal control analysis from the knowledge of the design temperature distributions on surface S_q, we consider the following two numerical test cases with different design temperature distributions.

One of the advantages of using the SDM is that the initial guesses of the unknown control function $\bar{h}_w(t)$ can be chosen arbitrarily. In all of the test cases considered here, the initial guesses for $\bar{h}_w(t)$ used to begin the iteration are taken as the normal working condition, $\bar{h}_w^0(t) = 20{,}000$ W/(m^2 · K). The heat transfer coefficient for normal working conditions is actually calculated based on the empirical equation proposed by Abadzic[13] with fluid velocity $V = 2.6$ m/s.

Because of the singularity of the gradient at final time, the estimated control functions at the last two time intervals are discarded, and, therefore, the effective optimal heat transfer coefficient is shown only up to $t = 35$s.

We now present two numerical experiments to determine $\bar{h}_w(t)$ by the optimal control analysis.

A. Numerical Test Case 1

The three-dimensional model of the motor housing is first solved for temperature distributions by using the normal working conditions with the data given earlier. The temperature distribution with time at four specified points (as shown in Fig. 3), from P_1 to P_4 on S_q, is shown as the original temperature distribution (solid line) in Fig. 4.

The rule of assigning the design temperature distributions is as follows: It is required that all of the temperatures on the heating surface be decreased by 5 K after time $t = 19$ s. The dashed line shown in Fig. 4 indicates the design temperature distribution with time P_1–P_4. The corresponding optimal control function is to be estimated such that the computed temperatures match as closely as possible the design temperatures on S_q.

The optimal control algorithm is, thus, performed in accordance with the preceding requirements. For the present optimization problem, the value of the functional cannot be decreased to a very small number because no solutions will match exactly the desired temperature distribution. Only the best or optimal solutions exist. For this reason, the stopping criterion is given by numerical observation; that is, when the value of functional cannot be further decreased, its value is chosen as the stopping criteria.

When the stopping criteria is set at $\varepsilon = 45{,}000$, after 14 iterations the optimal solutions converged. The estimated effective optimal heat transfer coefficient is shown in Fig. 5, and the corresponding estimated temperatures are shown in Fig. 4. It can be found from Fig. 4 that the design and estimated optimal temperature distributions are in a very good agreement at $P_3 \cdot P_2$ has the second best agreement, whereas P_1 has the worst agreement. This is because P_3 is located very close to the cooling passage, where the response

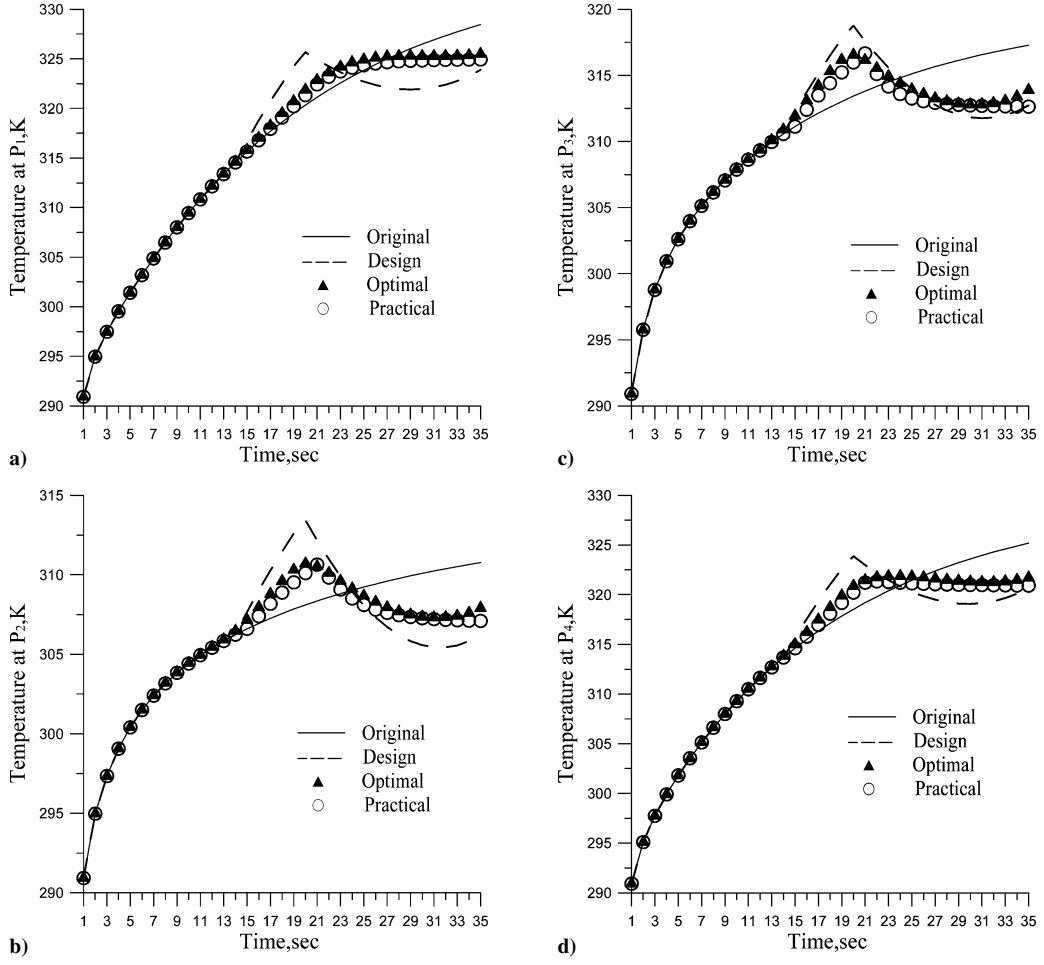

Fig. 9 Temperature distributions with time at a) P_1, b) P_2, c) P_3, and d) P_4 in case 2.

of the temperatures to the change of control function is very quick. However, the position of P_1 is located between two cooling passages; therefore, it has a very slow response to the change of the heat transfer coefficient, and this is why it has the highest temperatures in the entire housing domain.

The estimated effective optimal heat transfer coefficient is indeed the optimal control function because the relative error between the design and calculated (using the effective optimal control function) temperatures on the heating surface S_q is calculated as ERR = 4.02% (using degrees Celsius) or 0.48% (using Kelvin), where ERR is defined as

$$\text{ERR}\,\% = \left[\sum_{t=1}^{35} \sum_{e=1}^{E} \left| \frac{T_e(S_q, t) - Y_e(S_q, t)}{Y_e(S_q, t)} \right| \right] \div (E \times 35) \times 100\% \tag{16}$$

Here t represents the index of discreted time and $E = 600$ indicates the total number of design temperature indicating points on S_q.

The preceding test case seems unrealistic because it is impossible to generate such a control function in practice. For this reason, a step function approximation is used to average the values of the effective optimal control function and to obtain an effective practical heat transfer coefficient. This effective practical control function is shown in Fig. 5 (solid line). The corresponding temperatures based on this effective practical heat transfer coefficient are shown in Fig. 4. Note from Fig. 4 that the temperature distributions calculated by using the effective optimal and practical control functions are almost identical. This implies that the practical control function can, thus, be used in the realistic situation because it can be generated easily and the results are also reliable. In Fig. 5 the heat transfer coefficient goes up to about 70,000 W/(m^2 · K). If the fluid velocity cannot reach such a high $\bar{h}_w(t)$, this implies that the desired temperature distribution should be required to be higher.

The corresponding original, design, and estimated (using the effective practical control function) temperature distributions on the internal surface S_i at time $t = 30$ and 35 s are shown in Figs. 6 and 7, respectively. The relative error between the design and calculated (using the effective practical control function) temperatures on the heating surface S_q is calculated as ERR = 4.38% (using degrees Celsius) or 0.53% (using Kelvin). The external temperature distributions for the motor housing at $t = 35$ s are also shown in Fig. 8. Note that the temperature is always lower when there is a cooling passage passing through.

When the variation of cooling water temperature with time is considered, the capability of the proposed algorithm remains the same. However, a higher heat transfer coefficient will be obtained.

It can be learned based on the preceding numerical results that the calculated temperatures are still reliable, that is, close to the design temperatures, when using the effective practical heat transfer coefficient.

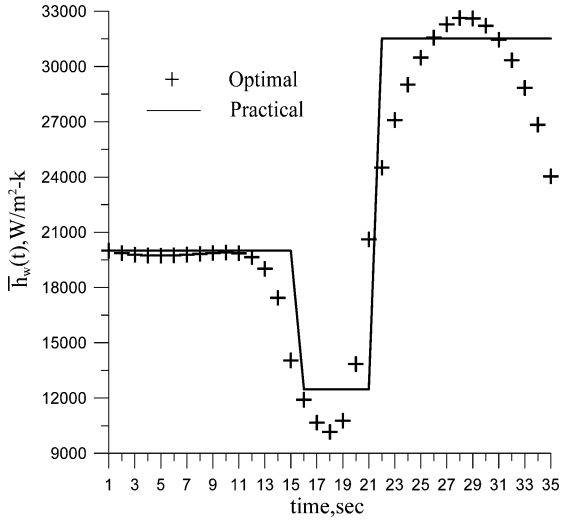

Fig. 10 Estimated effective optimal and practical heat transfer coefficients with time in case 2.

B. Numerical Test Case 2

The temperature distributions of the motor housing found by using the normal working conditions are the same as in test case 1. The original temperature distributions with time at P_1–P_4 on S_q are shown as the solid line in Fig. 9, where P_1 is the location with the highest temperature distribution in the entire domain.

The rule of assigning the design temperature distributions is as follows: It is required that all of the temperatures on the heating surface after time $t = 15$ s be added by the following function:

$$f(t) = 270 + 4.16 \times t - 0.068 \times t^2 \text{ K}, \qquad 15 \le t < 21 \text{ s}$$

$$f(t) = 366 - 3.1 \times t + 0.054 \times t^2 \text{ K}, \qquad 21 \le t \le 37 \text{ s} \tag{17}$$

which shows that the temperatures on the heating surface are first required to decrease. Then, after $t = 21$ s, the temperatures are required to increase. The dashed line in Fig. 9 indicates the design temperature distribution from time P_1 to P_4. It is hoped that the calculated temperatures using the effective control function be as close as possible to the design temperatures on S_q.

By the assignment of the stopping criteria $\varepsilon = 49{,}000$, the optimization analysis was performed. After only five iterations the solutions converged. The estimated effective optimal heat transfer

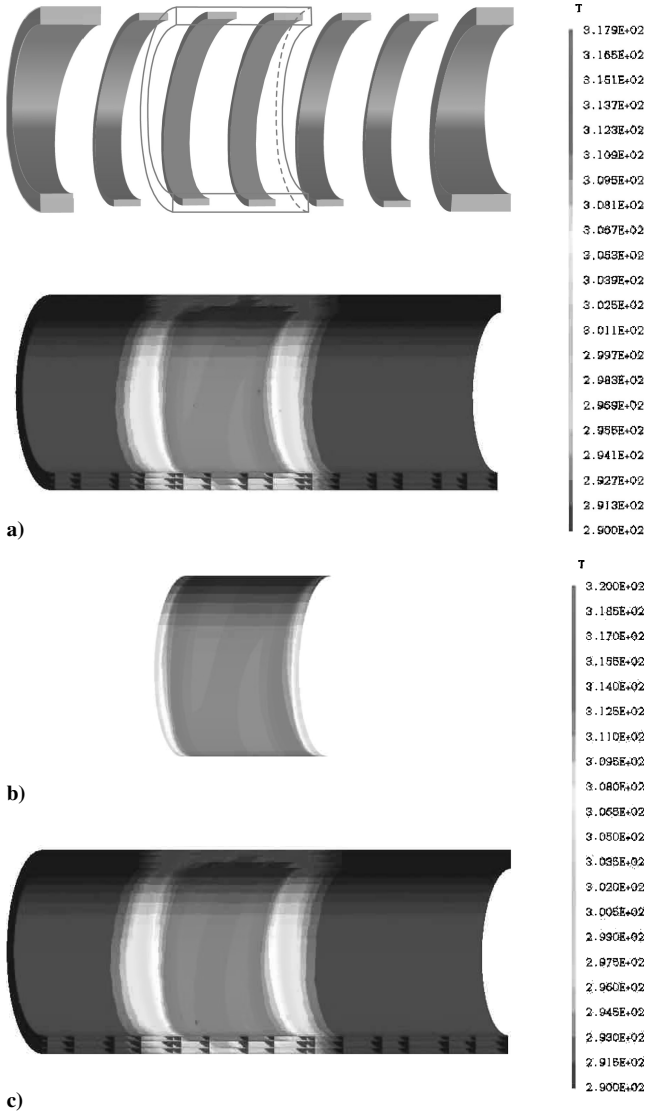

Fig. 11 Temperature distributions on internal surface of left housing at $t = 16$ s in case 2: a) original, b) design, and c) practical.

coefficient is shown in Fig. 10, and the corresponding estimated temperatures from P_1 to P_4 are also shown in Fig. 9. It is clear that the design and estimated temperature distributions using the optimal control function are in very good agreement at P_3. P_2 still has the second best agreement, and P_1 has the worst agreement. The reason is stated earlier in test case 1.

The estimated effective optimal heat transfer coefficient is indeed the optimal control function because the relative error between the design and calculated (using the effective optimal control function) temperatures on the heating surface S_q using both degrees Celsius and Kelvin are calculated as ERR = 3.50% and 0.46%, respectively.

Next, a step function approximation is used to average the values of the effective optimal control function, and then an effective practical heat transfer coefficient is obtained. This effective practical control function is shown in Fig. 10 (solid line). The corresponding calculated temperatures based on the effective practical heat transfer coefficient are shown in Fig. 9. Note from Fig. 9 that the temperature distributions calculated using the optimal and practical control functions are almost identical. This implies again that the substitution of a practical control function can still obtain reliable solutions.

The corresponding original, design, and estimated (using the effective practical control function) temperature distributions on the internal surface S_i at time $t = 16$ and 35 s are shown in Figs. 11 and 12, respectively. The relative error between the design and calculated (using the effective practical control function) temperatures on heating surface S_q using both degrees Celsius and Kelvin are calculated as ERR = 3.93% and 0.53%, respectively. The external temperature distributions for the motor housing at $t = 35$ s are shown in Fig. 13.

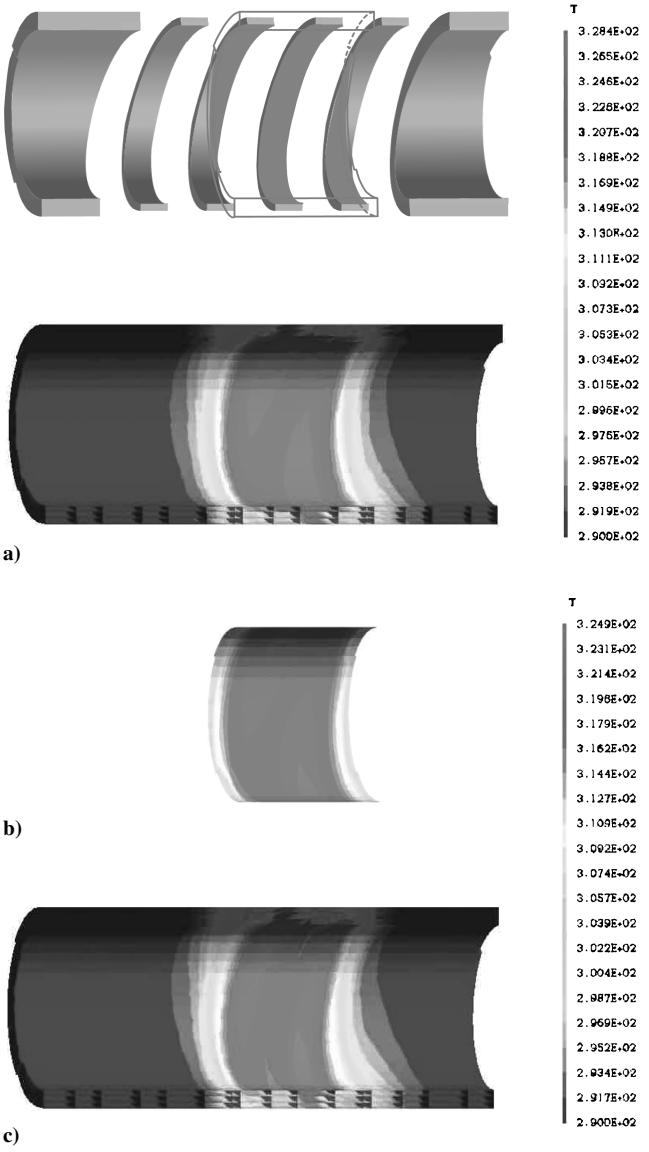

Fig. 12 Temperature distributions on internal surface of right housing at $t = 35$ s in case 2: a) original, b) design, and c) practical.

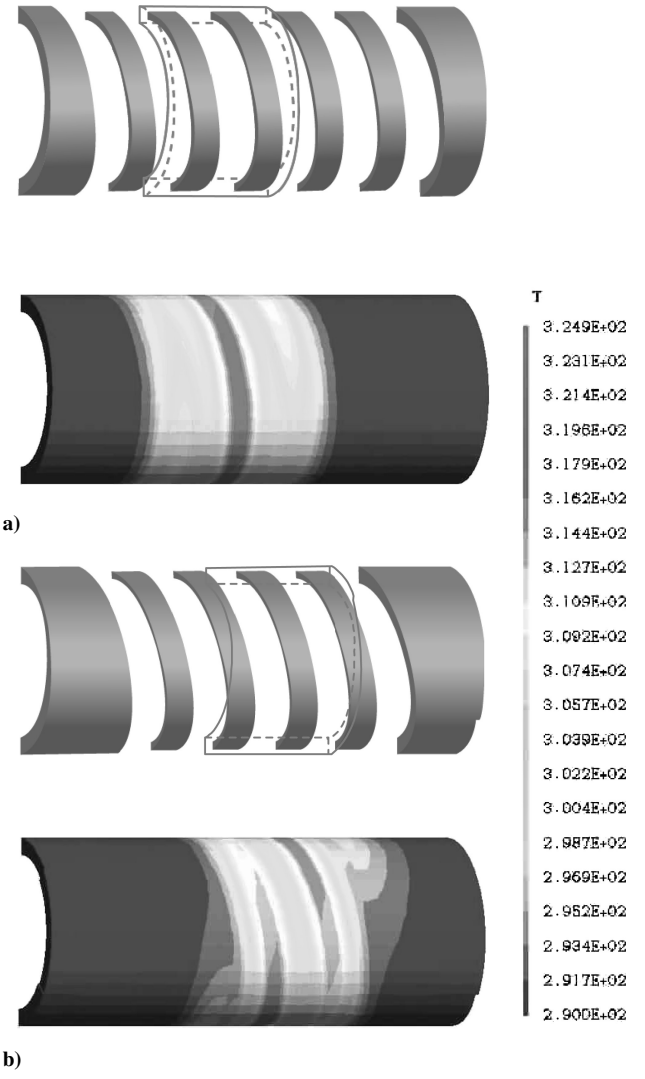

Fig. 13 External temperature distributions for a) left and b) right housing at $t = 35$ s in case 2.

It can be concluded from the foregoing two numerical test cases that the SDM has now been applied successfully in this three-dimensional optimal control problem for predicting the time-dependent effective heat transfer coefficient of the cooling passage for the motor housing.

VII. Conclusions

The SDM with an adjoint equation was successfully applied in predicting both the time-dependent effective optimal and practical heat transfer coefficients for a motor housing in a three-dimensional optimal control problem. Two test cases involving different design temperature distributions on the heating surface were considered. The results show that the SDM does not require a priori information for the functional form of the unknown functions and that reliable control functions can always be obtained.

Acknowledgment

This work was supported in part through the National Science Council, Republic of China, Grant NSC-93-2611-E-006-015.

References

[1]Bossmanns, B., and Tu, J. F., "A Thermal Model for High Speed Motorized Spindles," *International Journal of Machine Tools and Manufacture*, Vol. 39, No. 9, 1999, pp. 1345–1366.

[2]Yang, S. H., Kim, K. H., and Park, Y. K., "Measurement of Spindle Thermal Errors in Machine Tool Using Hemispherical Ball Bar Test," *International Journal of Machine Tools and Manufacture*, Vol. 44, No. 2-3, 2004, pp. 333–340.

[3]Chen, J. S., and Hsu, W. Y., "Characterizations and Models for the Thermal Growth of a Motorized High Speed Spindle," *International Journal of Machine Tools and Manufacture*, Vol. 43, No. 11, 2003, pp. 1163–1170.

[4]Ohishi, S., and Matsuzaki, Y., "Experimental Investigation of Air Spindle Unit Thermal Characteristics," *Journal of the International Societies for Precision Engineering and Nanotechnology*, Vol. 26, No. 1, 2002, pp. 49–57.

[5]Meric, R. A., "Finite Element Analysis of Optimal Heating of a Slab with Temperature Dependent Thermal Conductivity," *International Journal of Heat and Mass Transfer*, Vol. 22, No. 9, 1979, pp. 1347–1353.

[6]Meric, R. A., "Finite Element and Conjugate Gradient Methods for a Nonlinear Optimal Heat Transfer Control Problem," *International Journal for Numerical Methods in Engineering*, Vol. 14, No. 12, 1979, pp. 1851–1863.

[7]Chen, C. J., and Ozisik, M. N., "Optimal Heating of a Slab with a Plane Heat Source of Timewise Varying Strength," *Numerical Heat Transfer*, Pt. A, Vol. 21, No. 4, 1992, pp. 351–361.

[8]Chen, C. J., and Ozisik, M. N., "Optimal Heating of a Slab with Two Plan Heat Sources of Timewise Varying Strength," *Journal of the Franklin Institute*, Vol. 329, No. 3, 1992, pp. 195–206.

[9]Chen, C. J., and Ozisik, M. N., "Optimal Convective Heating of a Hollow Cylinder with Temperature Dependent Thermal Conductivity," *Applied Scientific Research*, Vol. 52, No. 2, 1994, pp. 67–79.

[10]Huang, C. H., "A Non-Linear Optimal Control Problem in Determining the Strength of the Optimal Boundary Heat Fluxes," *Numerical Heat Transfer*, Pt. B, Vol. 40, No. 5, 2002, pp. 411–429.

[11]Huang, C. H., and Li, C. Y., "A Three-Dimensional Optimal Control Problem in Determining the Boundary Control Heat Fluxes," *Heat and Mass Transfer*, Vol. 39, No. 7, 2003, pp. 589–598.

[12]Alifanov, O. M., *Inverse Heat Transfer Problems*, Springer-Verlag, Berlin, 1994, Chap. 8.

[13]Abadzic, E. E., "Heat Transfer on Coiled Tubular Matrix," American Society of Mechanical Engineers Paper 74-WA/HT-64, Feb. 1974.